Neurobiology of Disease 189 (2023) 106354

Contents lists available at ScienceDirect

Neurobiology of Disease

journal homepage: www.elsevier.com/locate/ynbdi

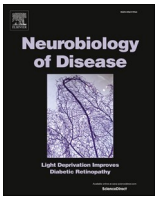

Gray matter structural covariance networks patterns associated with autopsy-confirmed LATE-NC compared to Alzheimer's disease pathology

Kaicheng Li [a,1], Xiao Luo [a,1], Qingze Zeng [a,1], Xiaocao Liu [a], Jixuan Li [a], Siyan Zhong [b], Xinyi Zhang [b], Xiaopei Xu [a], Shuyue Wang [a], Hui Hong [a], Yerfan Jiaerken [a], Zhirong Liu [b], Shuai Zhao [b], Peiyu Huang [a], Minming Zhang [a,**], Yanxing Chen [b,*], for the Alzheimer's Disease Neuroimaging Initiative[2]

[a] Department of Radiology, 2nd Affiliated Hospital of Zhejiang University School of Medicine, Hangzhou, China
[b] Department of Neurology, 2nd Affiliated Hospital of Zhejiang University School of Medicine, Hangzhou, China

ARTICLE INFO

Keywords:
LATE-NC
Limbic TDP-43
Alzheimer's disease
Mixed pathology
Gray matter structural covariance
Autopsy

ABSTRACT

Background: Cases with the limbic-predominant age-related TAR DNA-binding protein 43 (TDP-43) encephalopathy neuropathologic change (LATE-NC), Alzheimer's disease (AD), and mixed AD+TDP-43 pathology (AD+LATE-NC) share similar symptoms, which makes it a challenge for accurate diagnosis. Exploring the patterns of gray matter structural covariance networks (SCNs) in these three types may help to clarify the underlying mechanism and provide a basis for clinical interventions.

Methods: We included ante-mortem MRI data of 10 LATE-NC, 39 AD, and 25 AD+LATE-NC from the ADNI autopsy sample. We used four regions of interest (left posterior cingulate cortex, right entorhinal cortex, frontoinsular and dorsolateral prefrontal cortex) to anchor the default mode network (DMN), salience network (SN), and executive control network (ECN). Finally, we assessed the SCN alternations using a multi-regression model-based linear-interaction analysis.

Results: Cases with autopsy-confirmed LATE-NC and AD showed increased structural associations involving DMN, ECN, and SN. Cases with AD+LATE-NC showed increased structural association within DMN while decreased structural association between DMN and ECN. The volume of peak clusters showed significant associations with cognition and AD pathology.

Conclusions: This study showed different SCN patterns in the cases with LATE-NC, AD, and AD+LATE-NC, and indicated the network disconnection mechanism underlying these three neuropathological progressions. Further, SCN may serve as an effective biomarker to distinguish between different types of dementia.

Abbreviations: AD, Alzheimer's disease; LATE, limbic-predominant age-related TDP-43 encephalopathy; LATE-NC, the limbic-predominant age-related TDP-43 encephalopathy neuropathologic change; GM, gray matter; SCN, structural covariance network; DMN, default mode network; ECN, executive control network; ADNI, Alzheimer's disease Neuroimaging Initiative; HC, healthy control; MMSE, Mini-Mental State Examination; CDR, Clinical Dementia Rating; WMS-LM, Wechsler Memory Scale Logical Memory; GDS-15 score, Geriatric Depression Scale-15; ADNC, Alzheimer's disease neuropathologic change; Aβ, amyloid-β; SUVR, standardized uptake value ratio; TR, repetition time; TE, echo time; CAT12, Computational Anatomy Toolbox; TPM, tissue probability maps; WM, white matter; CSF, cerebrospinal fluid; ROIs, regions of interest; SN, salience network; GRF, Gaussian random field correction; APOE, Apolipoprotein E; EC, entorhinal cortex; PCC, posterior cingulate cortex; FIC, frontoinsular cortex; DLPFC, dorsolateral prefrontal cortex; HS, hippocampal sclerosis.

* Corresponding author at: Department of Neurology, The Second Affiliated Hospital, School of Medicine, Zhejiang University, 88 Jiefang Rd, Hangzhou 310009, China.

** Corresponding author.

E-mail address: chenyanxing@zju.edu.cn (Y. Chen).

[1] These authors contributed equally to this work.

[2] Data used in the preparation of this article were obtained from the Alzheimer's disease Neuroimaging Initiative (ADNI) database (http://www.adni.loni.usc.edu). As such, the investigators within the ADNI contributed to the design and implementation of ADNI and provided data but did not participate in analysis or writing of this report. A complete listing of ADNI investigators can be found at http://adni.loni.usc.edu/wp-content/up loads/how to apply/ADNI Acknowledgement List.pdf.

https://doi.org/10.1016/j.nbd.2023.106354
Received 27 August 2023; Received in revised form 14 November 2023; Accepted 14 November 2023
Available online 15 November 2023

1. Introduction

Alzheimer's disease (AD) is the most common form of dementia, but several other neurodegenerative pathologies may also result in similar clinical syndromes (Mehta and Schneider, 2021). One of the most common pathologies is limbic TAR DNA-binding protein 43 (TDP-43) proteinopathy, which has recently been categorized as a novel dementia subtype called limbic-predominant age-related TDP-43 encephalopathy (LATE) (Nelson et al., 2019; Katsumata et al., 2020). Clinically, LATE is easily confused with AD because of the considerable overlap of cognitive symptoms, showing more memory loss with relative sparing of executive functions (Kapasi et al., 2020). Moreover, autopsy series have estimated that LATE neuropathologic change (LATE-NC) can be detected in up to 57% of AD cases (Josephs et al., 2014; Josephs et al., 2008; Robinson et al., 2018), which can be defined as cases with mixed AD+TDP-43 pathology (AD+LATE-NC). Epidemiological studies found that these three pathological types (LATE-NC, AD, and AD+LATE-NC) featured various clinical progression (Meneses et al., 2021). Specifically, LATE-NC cases show a slower global cognitive decline than AD, while AD+LATE-NC cases show severer cognitive impairment. However, the LATE-NC can only be confirmed by autopsy. Exploring the neuroimaging changes can not only reflect the underlying mechanism corresponding to clinical manifestations but also find an imaging marker for disease diagnosis.

The neuroimaging analysis found different gray matter (GM) atrophy patterns in these three pathological types. For example, LATE-NC was found to be associated with widespread medial temporal lobe (MTL) atrophy (Wisse et al., 2021), especially in hippocampal subfields (Heywood et al., 2022; Josephs et al., 2017). Moreover, other studies found a distinct pattern of basal forebrain atrophy associated with LATE-NC compared to AD pathology (Teipel and Grothe, 2023; Makkinejad et al., 2019). Considering the network-like distribution patterns of LATE-NC and AD pathology, network analysis may be a proper method to reflect the GM changes (Meneses et al., 2021; Brier et al., 2016). GM structural covariance network (SCN) analysis is based on the findings that related regions co-vary in morphometric characteristics and could effectively measure the topographical organization (Alexander-Bloch et al., 2013; Bassett and Bullmore, 2009; Gong et al., 2012). The structural covariance patterns are associated with structural or functional connectivity (Alexander-Bloch et al., 2013). Thereinto, stronger covariance strength between seed and peak clusters indicates more network connections (Lin et al., 2016). Many previous studies focusing on AD found some meaningful results. For example, one SCN study found abnormal structural connectome even at the early stage of AD, suggesting its potential function as an early neuroimage biomarker (Montembeault et al., 2016). Moreover, several studies suggested AD patients with different genotypes would have different SCN patterns involving default mode network (DMN) and executive control network (ECN) (Chang et al., 2018; Chang et al., 2017). Thereinto, DMN is always the first target to be attacked, while ECN is usually initiated as compensation. Thus, exploring the different SCN patterns of the LATE-NC, AD, and AD+LATE-NC cases may clarify the underlying mechanism and provide some hints for clinical intervention.

Accordingly, we aimed to explore the patterns of SCNs in the cases with LATE-NC, AD, and AD+LATE-NC. We included ante-mortem MRI data of 10 LATE-NC, 39 AD, and 25 AD+LATE-NC from the ADNI autopsy sample. According to the previous studies of the clinical symptoms, we assumed that these three pathological types showed different SCN patterns, with more extensive SCN impairments in AD+LATE-NC cases.

2. Methods and materials

2.1. Alzheimer's disease neuroimaging and initiative

Data used in the preparation of this article were obtained from the Alzheimer's disease Neuroimaging Initiative (ADNI) database (http://adni.loni.usc.edu). The ADNI was initially launched in 2004 (ADNI-1), and additional recruitment was made through ADNI-GO in 2009, ADNI-2 in 2010, and ADNI-3 in 2016. The primary goal of ADNI has been to identify serial MRI, PET, biomarkers and genetic characteristics that would support the early detection and tracking of AD, and improved clinical trial design. For up-to-date information, see http://www.adni-info.org.

2.2. Study participants

We included the last available MRI scans of 74 ADNI subjects who had come to autopsy between 2007 and 2021. Moreover, we also included 71 healthy control (HC) from ADNI who were amyloid negative as the comparison (Flowchart in Supplementary Material 1) (Teipel and Grothe, 2022).

The inclusion criteria for HC included: (a) having a Mini-Mental State Examination (MMSE) between 24 and 30 (inclusive); (b) having a Clinical Dementia Rating (CDR) score of 0; (c) having a normal Wechsler Memory Scale Logical Memory (WMS-LM), delay recall performance (in detail: $\geq$9 for subjects with 16 or more years of education; $\geq$5 for subjects with 8–15 years of education; and $\geq$3 for 0–7 years of education); (d) non-clinical depression (Geriatric Depression Scale-15, GDS-15 score $<$ 6) (Sheikh, 1986); and (e) non-demented.

2.3. Neuropathological assessments

All neuropathological assessments are performed through the central laboratory of the ADNI neuropathology core (http://adni.loni.usc.edu/about/#core-container) (Josephs et al., 2017). The neuropathological results were captured in the format of the Neuropathology Data Form Version 11 of the National Alzheimer Coordinating Center.

We applied established rating scales for the presence of TDP-43 pathology and AD pathology, respectively. Specifically, the TDP-43 sum score was calculated by counting the total score across in amygdala, hippocampus, entorhinal/inferior temporal cortex or neocortex, while AD pathology was reflected using NIA-AA Alzheimer's disease neuropathologic change (ADNC) score. Cases were classified as LATE-NC if they had a TDP-43 sum score of 2 or higher and an ADNC score of below 2, indicating no or low presence of AD pathology. By contrast, cases were classified as AD if they had an ADNC score of 2 or higher, indicating at least moderate presence of AD pathology, and a TDP-43 sum score of 0, indicating no TDP-43 pathology in any of the four regions. Cases were classified as AD+LATE-NC if the TDP-43 sum score was $\geq$2 and the ADNC score was $\geq$2.

Finally, from the 74 cases available, we identified 10 cases with LATE-NC, 39 cases with AD, and 25 cases with AD+LATE-NC.

2.4. Neuropsychological assessment and PET data acquisition

All subjects underwent comprehensive neuropsychological tests, including an assessment of general mental status (MMSE; CDR) and other cognitive domains, including memory function, executive function, language ability, and visuospatial function. We included the last available neuropsychological tests of 74 ADNI subjects who had come to autopsy between 2007 and 2021.

We used the amyloid-β (Aβ) PET standardized uptake value ratio (SUVR) to reflect AD pathological burden. Global Aβ values were determined for each subject by calculating a non-weighted average uptake across the frontal, anterior/posterior cingulate, lateral parietal, and lateral temporal lobes (segmented by Freesurfer) and dividing this average by the whole cerebellum uptake. The cutoffs to define Aβ positivity were based on previous studies: SUVR$\geq$1.11 for [18F]-AV45 PET (Landau et al., 2012).

2.5. MRI acquisition and pre-processing

MRI data were acquired in 3 T scanners. Briefly, the ADNI protocol includes T1-weighted acquisition based on a sagittal volumetric magnetization-prepared rapid gradient echo sequence collected from a variety of MR systems with protocols optimized for each type of scanner. Representative imaging parameters were as follows: repetition time (TR) =7 ms; echo time (TE) =3 ms; within plane FOV = 256 × 256 mm^2; voxel size = 1.1 × 1.1 × 1.2 mm^3; flip angle = 9° or 11°.

We pre-processed all T1-weighted images using the Computational Anatomy Toolbox (CAT12, http://dbm.neuro.uni-jena.de/cat12/) toolbox segment data pipeline implemented within SPM12 in Matlab (R2022). First, the T1 image was spatially registered to the tissue probability maps (TPM) and then segmented into GM, white matter (WM) and cerebrospinal fluid (CSF). We performed the affine registration to the stereotactic MNI space using ICBM152 space. Second, we performed normalization and nonlinear modulation using the Jacobian determinants. To remove the MRI inhomogeneities and noise, we corrected the bias, noise and normalized the intensities. Subsequently, we smoothed the GM image with a Gaussian kernel of 8 mm × 8 mm × 8 mm to reduce potential inaccuracies during the normalization step. Moreover, we assessed processed image quality by visual inspection and weighted average image quality index. No subjects were excluded due to bad image quality.

2.6. Structural covariance gray matter network processing

To investigate the SCNs, we chose four regions of interest (ROIs) as previously (Montembeault et al., 2016): right entorhinal cortex (EC, MNI coordinates: 25, −9, −28) (Bernhardt et al., 2008; Eickhoff et al., 2005), left posterior cingulate cortex (PCC, MNI coordinates: −2, −36, 35) (Zielinski et al., 2012; Spreng and Turner, 2013), right frontoinsular cortex (FIC, MNI coordinates: 38, 26, −10), and right dorsolateral prefrontal cortex (DLPFC, MNI coordinates: 44, 36, 20) (Montembeault et al., 2016; Zielinski et al., 2010). These regions respectively anchor the DMN medial temporal subsystem, DMN midline core subsystem, salience network (SN) and ECN.

To achieve SCN t-maps, we performed the general linear analysis on modulated GM images. Specifically, we extracted the GM volume from a 4-mm radius sphere (Montembeault et al., 2016; Chang et al., 2018; Chang et al., 2017) around those coordinates on modulated images. Then, we performed four separate correlation analyses by entering the GM volumes of each ROI as a regressor and the total intracranial volume, gender, age, and education as covariates. We performed Fisher's Z transformation before statistical correction.

First, we performed specific contrasts within each group to identify voxels expressing a positive correlation with each ROI. We set the threshold at $P \leq 0.05$ at the voxel level and cluster size>100, uncorrected. To achieve group-wise comparisons, we displayed the results on a standard brain template (ICBM152).

Then, we used multi-regression model-based linear interaction analysis (Bernhardt et al., 2008) to assess SCN alternations between groups by setting the threshold at minimum $Z > 2.3$; cluster significance: $P < 0.05$, Gaussian random field correction (GRF) corrected. Subsequently, we explored: (1) the associations between cognition and the identified peak voxel volume; and (2) the associations between pathologies and the identified peak voxel volume (by extracting the GM volume using a 4-mm radius sphere).

3. Results

3.1. Demographics

Demographics of three pathological types and amyloid-negative HC are displayed in Table 1. To be specific, cases with AD, LATE-NC, and AD+LATE-NC matched well with HC on age, gender, and education ($P > 0.05$). Cases with AD and AD+LATE-NC had a significantly higher prevalence of the Apolipoprotein E (APOE) ε4 genotype as compared with HC. Cases with AD, LATE-NC, and AD+LATE-NC showed worse cognition (including MMSE, CDR, memory, executive function, language) than HC. Notably, cases with LATE-NC showed a relatively lower prevalence of the APOE ε4 and better cognition (CDR, memory, and executive function) than cases with AD and AD+LATE-NC.

Table 1
Demographic and neuropsychological data.

Demographic characteristics	HC N = 71	AD N = 39	LATE-NC N = 10	AD + LATE-NC N = 25	P-value
Age of scan, y, mean ± SD	75.19 ± 4.41	75.44 ± 7.45	78.45 ± 5.00	77.38 ± 7.14	0.200
Age of death, y, mean ± SD	NA	81.33 ± 7.15	85.50 ± 6.13	84.48 ± 6.92	0.104
interval, y, mean ± SD	NA	5.90 ± 3.54	7.05 ± 3.21	7.10 ± 2.83	0.302
Female, n(%)	30/71	10/39	2/8	6/25	0.146
Education,y, mean ± SD	16.70 ± 2.57	16.74 ± 2.48	15.90 ± 2.73	15.64 ± 3.13	0.282
APOE ε4 allele	13/71 (18.30%)	30/39 (76.9%)	1/10 (10.0%)	17/25 (68.0%)	<0.001[acdf]
GDS	0.62 ± 1.07	1.44 ± 1.47	1.10 ± 1.73	1.60 ± 1.32	0.002[ac]
MMSE	28.86 ± 1.44	25.79 ± 2.81	27.20 ± 2.04	25.96 ± 2.46	<0.001[abc]
CDR global	0.00 ± 0.00	1.46 ± 0.85	1.05 ± 0.69	1.56 ± 0.85	<0.001[abcf]
CDR sum	0.00 ± 0.00	8.47 ± 5.14	5.65 ± 3.94	8.92 ± 5.03	<0.001[abcdf]
Memory	1.00 ± 0.57	−0.74 ± 0.95	−0.07 ± 0.69	−0.71 ± 0.73	<0.001[abcdf]
Executive function	0.85 ± 0.80	−1.00 ± 1.29	0.06 ± 1.09	−0.59 ± 1.04	<0.001[abcd]
Language	0.81 ± 0.71	−0.76 ± 1.40	−0.07 ± 1.09	−0.55 ± 0.94	<0.001[abc]
Visuospatial	0.10 ± 0.68	−0.62 ± 1.20	−0.09 ± 0.84	−0.43 ± 0.88	0.001[ac]

Data are presented as means±standard deviations.
HC: healthy control; LATE-NC: the limbic-predominant age-related TDP-43 encephalopathy neuropathologic change; TDP-43: transactive response DNA binding protein of 43 kDa; AD:Alzheimer's disease; AD+LATE-NC: mixed AD+TDP-43 pathology; APOE: Apolipoprotein E; GDS: Geriatric Depression Scale; MMSE: Mini-Mental State Examination; CDR: Clinical Dementia Rating.
a–fPost hoc analysis further revealed the source of ANOVA difference (a: HC VS. AD; b: HC VS. LATE-NC; c: HC VS. AD+LATE-NC; d: AD VS. LATE-NC; e: AD VS. AD+LATE-NC; f: LATE-NC VS. AD+LATE-NC) ($P < 0.05$, significant difference between groups).

3.2. Patterns of Structural Association within groups

To qualitatively compare the patterns of positive correlations in subjects of different groups, we presented the statistical brain maps in Fig. 1. In all SCNs (DMN, SN, and ECN), cases with AD presented a greater amount of voxels than HC and the other two types; cases with LATE-NC and AD+LATE-NC presented a less amount of voxels than HC.

3.3. The difference of structural covariance gray matter network

The LATE-NC cases showed: (1) increased structural associations between PCC (DMN midline core subsystem) and frontal regions as well as the hippocampus; (2) increased structural associations between FIC (SN) and temporal regions.

The AD cases showed: (1) increased structural associations between PCC (DMN midline core subsystem) and temporal regions; (2) increased structural associations between FIC (SN) and frontal regions.

The AD+LATE-NC cases showed: (1) decreased structural associations between EC (DMN medial temporal subsystem) and frontal

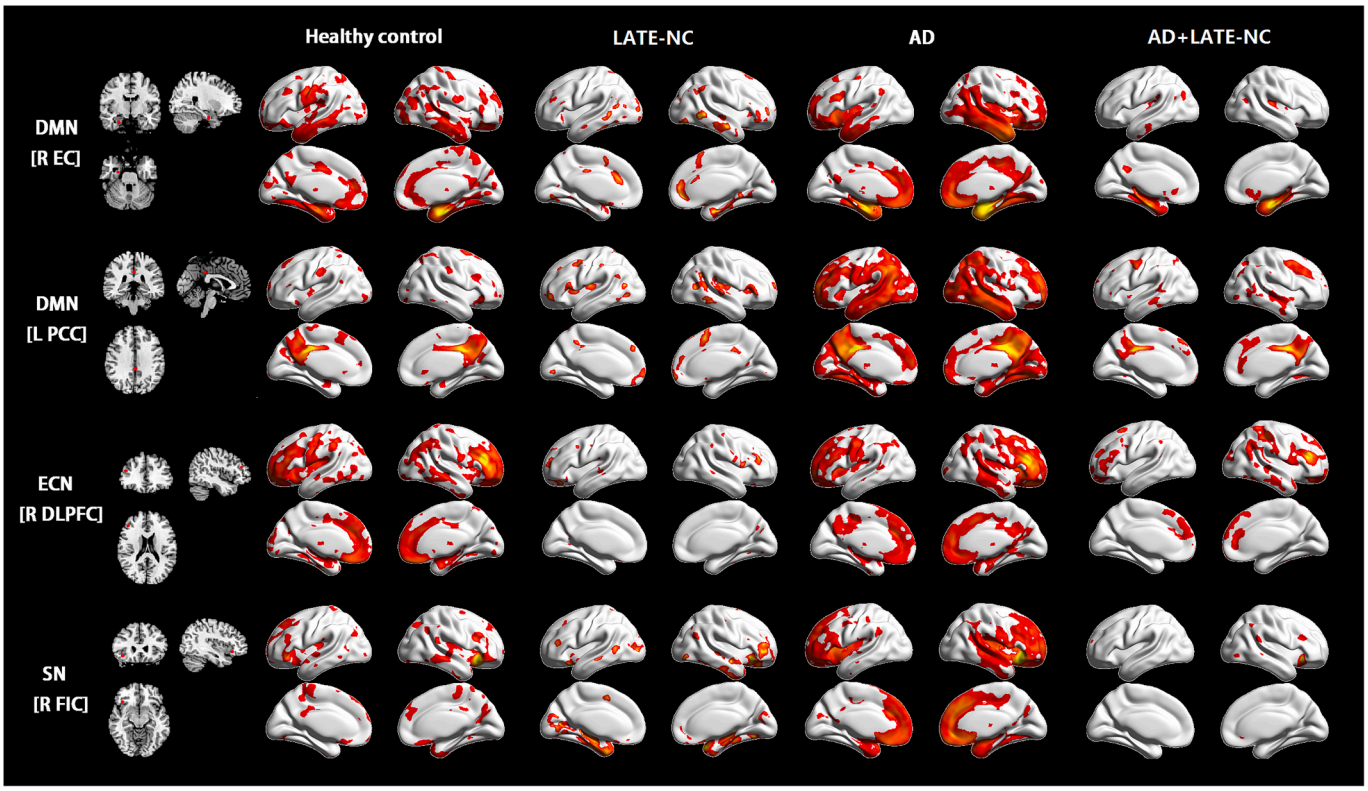

Fig. 1. Gray Matter Structural Covariance network within every group.
Abbreviation: LATE-NC: the limbic-predominant age-related TDP-43 encephalopathy neuropathologic change; TDP-43: transactive response DNA binding protein of 43 kDa; AD: Alzheimer's disease; AD+LATE-NC: mixed AD+TDP-43 pathology; DMN: default mode network; ECN: executive control network; SN: salience network; EC: entorhinal cortex; PCC: posterior cingulate cortex; DLPFC: dorsolateral prefrontal cortex; FIC: frontoinsular cortex; R: right; L: left

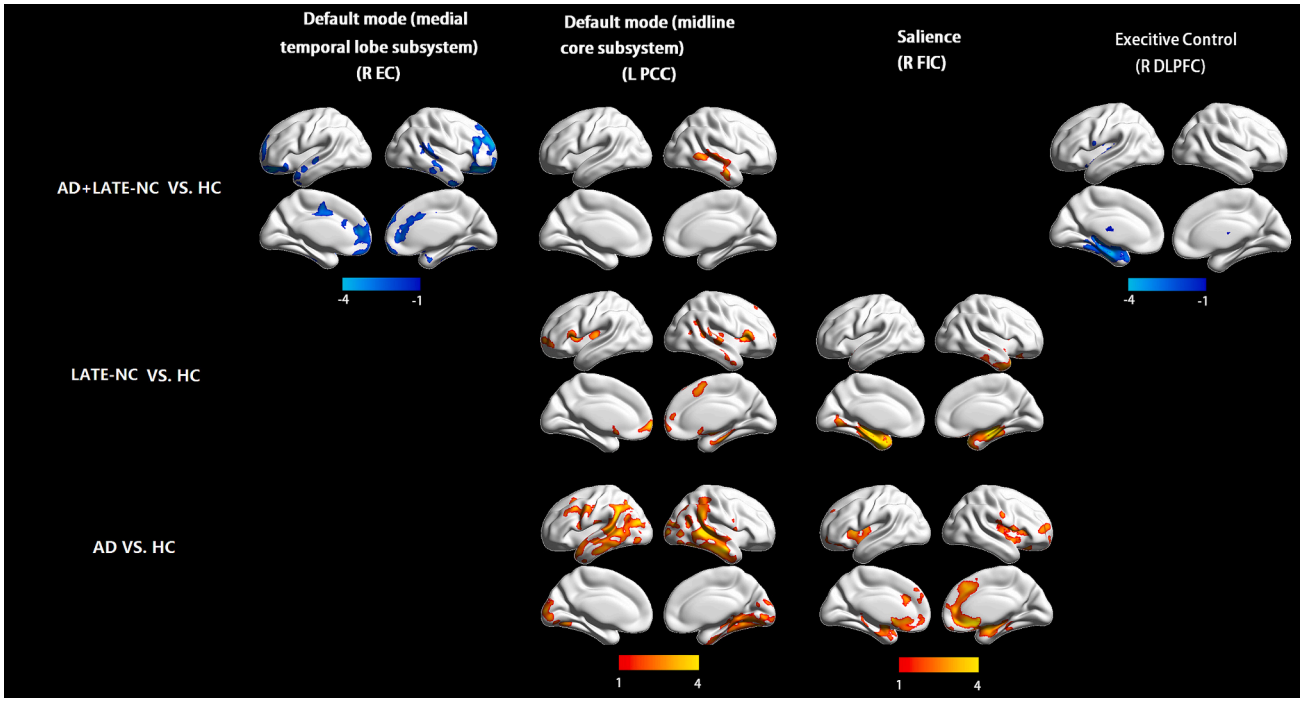

Fig. 2. The difference of Gray Matter Structural Covariance network between subjects in three pathological types and healthy control.
Abbreviations: EC: entorhinal cortex; PCC: posterior cingulate cortex; FIC: frontoinsular cortex; DLPFC: dorsolateral prefrontal cortex; LATE-NC: the limbic-predominant age-related TDP-43 encephalopathy neuropathologic change; TDP-43: transactive response DNA binding protein of 43 kDa; AD:Alzheimer's disease; AD+LATE-NC: mixed AD+TDP-43 pathology.

regions; (2) increased structural associations between PCC (DMN midline core subsystem) and temporal regions; (3) decreased structural associations between DLPFC (ECN) and fusiform.

Detailed information in Fig. 2 and Table 2. Additionally, to show the differences between cases with AD and AD+LATE-NC directly, we further performed the group comparisons between these two groups and added them in the Supplementary Material 2.

Additionally, we performed analyses using the contralateral ROI seeds by changing the sign on each seed's x coordinate (detailed information in Supplementary Material 3) (Zielinski et al., 2010).

3.4. Correlations of peak cluster volumes with neuropsychological and pathological scores

Firstly, we performed the correlation analysis between the peak cluster volumes and neuropsychological scores. The peak cluster positively correlated with cognition (MMSE, memory, executive function, and visuospatial function) and negatively correlated with CDR. Secondly, we performed the correlation analysis between the peak cluster volumes and pathological scores. In cases with AD, the peak volume of the left middle temporal gyrus negatively correlated with ADNC ($r = -0.35$, $P = 0.03$). In cases with AD+LATE-NC, the peak volume of left fusiform negatively correlated with ADNC ($r = -0.73$, $P < 0.01$). Detailed information can be found in Supplementary Material 4.

4. Discussion

The current study showed different patterns of SCN damage in cases with AD, LATE-NC, and AD+LATE-NC. To be specific, the cases with LATE-NC and AD exhibited increased structural associations involving DMN, ECN, and SN. However, the cases with AD+LATE-NC showed decreased structural association between DMN and ECN, as well as increased structural association within DMN. These SCNs changes were partially related to specific pathological distribution and can help to illuminate the cognitive changes.

The different pathological spread patterns of TDP-43 and AD pathologies are key underlying mechanisms. On the one hand, TDP-43 pathology spreads from the amygdala, EC, then to the inferior temporal cortex and insula, and finally reaches the middle frontal cortex (Meneses et al., 2021). This can partially explain the relatively smaller network range of LATE-NC cases in the current study since some cases had high TDP-43 scores, indicating the involvement of late-stage areas such as the insula and frontal lobes. And the relatively small sample size of the LATE-NC cases may be another reason. On the other hand, AD neuropathology accumulates in a specific temporal-ordered pattern (Sperling et al., 2014), with extracellular Aβ appearing at the earliest followed by intracellular phosphorylated tau deposition, and downstream neurodegeneration events (Jack Jr. et al., 2013).The observed smaller network range of AD+LATE-NC cases may be due to the coexistence of two pathologies and their interactions (Herman et al., 2011; Davis et al., 2017). To be specific, TDP-43 aggregates influence amyloid-beta plaque deposition and tau aggregation.

Cases with LATE-NC showed increased structural associations between SN and temporal regions, which may indicate the GM co-vary in these regions considering the distribution pattern of TDP-43 pathology (Meneses et al., 2021). Evidence comes from previous structural studies. For example, LATE-NC cases always showed MTL atrophy (Wisse et al., 2021), especially involving the hippocampus (Heywood et al., 2022; Josephs et al., 2017). Another study using multi-echo spin-echo MRI found that LATE-NC is associated with a lower R2 relaxation rate involving the temporal, frontal, and basal ganglia, indicating LATE-NC-associated neuronal damage (Tazwar et al., 2022). Moreover, since LATE-NC always coexists with hippocampal sclerosis (HS) (Nelson et al., 2019; Zarow et al., 2012), HS studies which reported the MTL atrophy can also partially support the current findings (Li et al., 2023; Dawe et al., 2020). One recent fluorodeoxyglucose positron emission tomography study found the specific temporolimbic-predominant neurodegeneration pattern in amnestic patients with limbic TDP-43 pathology and HS (Botha et al., 2018). On the other hand, cases with LATE-NC also showed increased structural associations between PCC and frontal regions as well as temporal regions. This is more likely to be a compensatory increase within network and between network associations. Further analysis showing the positive associations between peak cluster volume and cognition may also support this.

Cases with AD showed increased structural associations between PCC and temporal regions, indicating the GM co-vary. This matches the AD pathological distribution pattern: tau starting from EC and spreading posteriorly to the PCC, suggesting the GM synergistic atrophy within DMN due to pathological spread. Moreover, cases with AD also showed increased structural associations between SN and frontal regions, which may work as compensation under AD pathology. Similar results can be found in previous studies, showing that ECN was usually activated as a compensatory network in AD patients (Stern, 2006; Li et al., 2019). This may also help to explain why the cognitive performance is relatively

Table 2
The difference of gray matter structural covariance network between subjects in three pathological types and healthy control.

Network	Group	Cluster/peak regions	MNI coordinates			Extent	Max T
			X	Y	Z		
Default mode (medial temporal lobe subsystem) (R EC)	LATE-NC VS. HC	No					
	AD VS. HC	No					
	AD+LATE-NC VS. HC	R Inferior frontal gyrus, orbital part	34.5	34.5	−12	31,348	−5.105
		R Inferior frontal gyrus, triangular part	43.5	21	3	9311	4.515
		R Hippocampus	18	−13.5	−15	2170	4.151
Default mode (midline core subsystem) (L PCC)	LATE-NC VS. HC	L Superior frontal gyrus, medial orbital	−3	63	−3	3773	4.411
		L Inferior frontal gyrus, opercular part	−43.5	13.5	3	3222	4.763
		R Superior Frontal	13.5	30	48	1415	3.406
	AD VS. HC	R Middle Temporal	60	−43.5	4.5	31,424	4.947
		L Middle Temporal	−60	−58.5	30	20,678	4.588
	AD+LATE-NC VS. HC	R Middle Temporal	60	−9	−25.5	4705	3.476
Salience (R FIC)	LATE-NC VS. HC	L Inferior Temporal	−25.5	0	−42	8849	6.321
		R Hippocampus	28.5	−21	−9	11,236	5.750
	AD VS. HC	Medial Frontal Gyrus	28.5	−16.5	7.5	39,182	5.852
	AD+LATE-NC VS. HC	No					
Executive Control (R DLPFC)	LATE-NC VS. HC	No					
	AD VS. HC	No					
	AD+LATE-NC VS. HC	L Fusiform	−30	−16.5	−27	8600	−4.867

Abbreviations: HC: healthy control; EC: entorhinal cortex; PCC: posterior cingulate cortex; FIC: frontoinsular cortex; DLPFC: dorsolateral prefrontal cortex; LATE-NC: the limbic-predominant age-related TDP-43 encephalopathy neuropathologic change; TDP-43: transactive response DNA binding protein of 43 kDa; AD:Alzheimer's disease; AD+LATE-NC: mixed AD+TDP-43 pathology; R: right; L: left.

normal in the currently included cases with AD.

Cases with AD+LATE-NC showed increased structural associations between PCC and temporal regions. This is similar to the findings in cases with AD and LATE-NC, indicating a similar effect resulted from the two pathologies. Interestingly, we also observed decreased structural associations between ECN and DMN in cases with AD+LATE-NC, indicating that these GM changes asynchronously. This is different from what was observed in cases with only TDP-43 or AD pathology and may indicate the interaction effect. The coexistence of AD pathology and TDP-43 may exacerbate the damage to the neuron. Similar results can be found in previous studies (Meneses et al., 2021), AD patients with TDP-43 pathology have severer cognitive impairment compared to those without TDP-43 pathology.

Overall, this study highlights the importance of understanding the different patterns of brain damage in various pathologies and their implications for clinical manifestations. These findings may also provide some imaging evidence for future clinical treatments targeting AD pathology or TDP-43 pathology.

4.1. Limitation

There were some limitations to this study. Firstly, the sample size of cases with LATE-NC is relatively small, which may weaken the statistical effort. Further study with a bigger sample size should be performed. Moreover, our SCN analysis was constructed in a group level which limits the prediction of the pathology using single-subject gray matter network measures. Further SCN analysis based on single-subject should be done. Finally, more networks should be explored to show brain impairments underlying TDP-43 and AD pathologies in the future.

Ethics approval statement and patient consent statement

All procedures performed in studies involving human participants were in accordance with the ethical standards of the institutional and national research committee and with the 1964 Helsinki declaration and its later amendments or comparable ethical standards. Written informed consent was obtained from all participants and authorized representatives, and the study partners before any protocol-specific procedures were carried out in the ADNI study. More details can be found at http://www.adni-info.org.

Consent for publication

Not applicable.

Funding statement

This study was supported by the National Natural Science Foundation of China (Grant No. 82202090, 82371190 and 82271936), the China Postdoctoral Science Foundation (Grant No.2022M722751), Zhejiang medical and health science and technology project (Grant No.2023567844) and Zhejiang Provincial Natural Science Foundation of China (Grant No. LTGY23F010001), Zhejiang Provincial Traditional Chinese Medicine Science and Technology Program (Grant No. 2024ZL575).

Authors' contributions

KL, XL, XZ contributed equally to this work. KL designed the study and wrote the first draft of the manuscript. XL, XZ analyzed the MRI data and wrote the protocol. XL, JL collected clinical and MRI data. SZ, XZ, XX, SW, HH, JY, ZL, SZ, MZ, PH and YC assisted with study design and interpretation of findings. YC modified the expression and grammar thoroughly. All authors have contributed to and approved the final manuscript. All authors read and approved the final manuscript.

Permission to reproduce material from other sources

Not applicable.

Clinical trial registration

Not applicable.

Required financial disclosures

Not applicable.

Declaration of Competing Interest

The authors declare no conflict of interest.

Data availability

The datasets generated and analyzed during the current study are available in the ADNI study. More details in www.adni-info.org.

Acknowledgements

Not applicable.

Appendix A. Supplementary data

Supplementary data to this article can be found online at https://doi.org/10.1016/j.nbd.2023.106354.

References

Alexander-Bloch, A., Giedd, J.N., Bullmore, E., 2013. Imaging structural co-variance between human brain regions. Nat. Rev. Neurosci. 14, 322e36.
Bassett, D.S., Bullmore, E.T., 2009. Human brain networks in health and disease. Curr. Opin. Neurol. 22 (4), 340–347.
Bernhardt, B.C., Worsley, K.J., Besson, P., Concha, L., Lerch, J.P., Evans, A.C., et al., 2008. Mapping limbic network organization in temporal lobe epilepsy using morphometric correlations: insights on the relation between mesiotemporal connectivity and cortical atrophy. Neuroimage. 42 (2), 515–524.
Botha, H., Mantyh, W.G., Murray, M.E., Knopman, D.S., Przybelski, S.A., Wiste, H.J., et al., 2018. FDG-PET in tau-negative amnestic dementia resembles that of autopsy-proven hippocampal sclerosis. Brain. 141 (4), 1201–1217.
Brier, M.R.G.B., Friedrichsen, K., McCarthy, J., Stern, A., Christensen, J., Owen, C., Aldea, P., Su, Y., Hassenstab, J., Cairns, N.J., Holtzman, D.M., Fagan, A.M., Morris, J. C., Benzinger, T.L., Ances, B.M., 2016. Tau and Aβ imaging, CSF measures, and cognition in Alzheimer's disease. Sci. Transl. Med. 8 (338).
Chang, Y.T., Hsu, S.W., Tsai, S.J., Chang, Y.T., Huang, C.W., Liu, M.E., et al., 2017. Genetic effect of MTHFR C677T polymorphism on the structural covariance network and white-matter integrity in Alzheimer's disease. Hum. Brain Mapp. 38 (6), 3039–3051.
Chang, C.C., Chang, Y.T., Huang, C.W., Tsai, S.J., Hsu, S.W., Huang, S.H., et al., 2018. Associations of Bcl-2 rs956572 genotype groups in the structural covariance network in early-stage Alzheimer's disease. Alzheimers Res. Ther. 10 (1), 17.
Davis, S.A., Gan, K.A., Dowell, J.A., Cairns, N.J., Gitcho, M.A., 2017. TDP-43 expression influences amyloidβ plaque deposition and tau aggregation. Neurobiol. Dis. 103, 154–162.
Dawe, R.J., Yu, L., Arfanakis, K., Schneider, J.A., Bennett, D.A., Boyle, P.A., 2020. Late-life cognitive decline is associated with hippocampal volume, above and beyond its associations with traditional neuropathologic indices. Alzheimers Dement. 16 (1), 209–218.
Eickhoff, S.B., Stephan, K.E., Mohlberg, H., Grefkes, C., Fink, G.R., Amunts, K., et al., 2005. A new SPM toolbox for combining probabilistic cytoarchitectonic maps and functional imaging data. Neuroimage. 25 (4), 1325–1335.
Gong, G.H.Y., Chen, Z., Evans, A., 2012. Convergence and divergence of thickness correlations with diffusion connections across the human cerebral cortex. Neuroimage. 59, 1239–1248.
Herman, A.M., Khandelwal, P.J., Stanczyk, B.B., Rebeck, G.W., Moussa, C.E., 2011. β-Amyloid triggers ALS-associated TDP-43 pathology in AD models. Brain Res. 1386, 191–199.
Heywood, A., Stocks, J., Schneider, J.A., Arfanakis, K., Bennett, D.A., Beg, M.F., et al., 2022. The unique effect of TDP-43 on hippocampal subfield morphometry and cognition. Neuroimage Clin. 35, 103125.
Jack Jr., C.R., Knopman, D.S., Jagust, W.J., Petersen, R.C., Weiner, M.W., Aisen, P.S., et al., 2013. Tracking pathophysiological processes in Alzheimer's disease: an updated hypothetical model of dynamic biomarkers. Lancet Neurol. 12 (2), 207–216.

Josephs, K.A., Whitwell, J.L., Knopman, D.S., Hu, W.T., Stroh, D.A., Baker, M., et al., 2008. Abnormal TDP-43 immunoreactivity in AD modifies clinicopathologic and radiologic phenotype. Neurology. 70 (19 Pt 2), 1850–1857.
Josephs, K.A., Murray, M.E., Whitwell, J.L., Parisi, J.E., Petrucelli, L., Jack, C.R., et al., 2014. Staging TDP-43 pathology in Alzheimer's disease. Acta Neuropathol. 127 (3), 441–450.
Josephs, K.A., Dickson, D.W., Tosakulwong, N., Weigand, S.D., Murray, M.E., Petrucelli, L., et al., 2017. Rates of hippocampal atrophy and presence of post-mortem TDP-43 in patients with Alzheimer's disease: a longitudinal retrospective study. Lancet Neurol. 16 (11), 917–924.
Kapasi, A., Yu, L., Boyle, P.A., Barnes, L.L., Bennett, D.A., Schneider, J.A., 2020. Limbic-predominant age-related TDP-43 encephalopathy, ADNC pathology, and cognitive decline in aging. Neurology. 95 (14) e1951-e62.
Katsumata, Y., Abner, E.L., Karanth, S., Teylan, M.A., Mock, C.N., Cykowski, M.D., et al., 2020. Distinct clinicopathologic clusters of persons with TDP-43 proteinopathy. Acta Neuropathol. 140 (5), 659–674.
Landau, S.M., Mintun, M.A., Joshi, A.D., Koeppe, R.A., Petersen, R.C., Aisen, P.S., et al., 2012. Amyloid deposition, hypometabolism, and longitudinal cognitive decline. Ann. Neurol. 72 (4), 578–586.
Li, K., Luo, X., Zeng, Q., Huang, P., Shen, Z., Xu, X., et al., 2019. Gray matter structural covariance networks changes along the Alzheimer's disease continuum. Neuroimage Clin. 23, 101828.
Li, J.X., Nguyen, H.L., Qian, T., Woodworth, D.C., Sajjadi, S.A., 2023. Longitudinal hippocampal atrophy in hippocampal sclerosis of aging. Aging Brain. 4, 100092.
Lin, P.H., Tsai, S.J., Huang, C.W., Mu-En, L., Hsu, S.W., Lee, C.C., et al., 2016. Dose-dependent genotype effects of BDNF Val66Met polymorphism on default mode network in early stage Alzheimer's disease. Oncotarget. 7 (34), 54200–54214.
Makkinejad, N., Schneider, J.A., Yu, J., Leurgans, S.E., Kotrotsou, A., Evia, A.M., et al., 2019. Associations of amygdala volume and shape with transactive response DNA-binding protein 43 (TDP-43) pathology in a community cohort of older adults. Neurobiol. Aging 77, 104–111.
Mehta, R.I., Schneider, J.A., 2021. What is 'Alzheimer's disease'? The neuropathological heterogeneity of clinically defined Alzheimer's dementia. Curr. Opin. Neurol. 34 (2), 237–245.
Meneses, A., Koga, S., O'Leary, J., Dickson, D.W., Bu, G., Zhao, N., 2021. TDP-43 Pathology in Alzheimer's Disease. Mol. Neurodegener. 16 (1), 84.
Montembeault, M., Rouleau, I., Provost, J.S., Brambati, S.M., Alzheimer's Disease Neuroimaging I, 2016. Altered gray matter structural covariance networks in early stages of Alzheimer's Disease. Cereb. Cortex 26 (6), 2650–2662.
Nelson, P.T., Dickson, D.W., Trojanowski, J.Q., Jack, C.R., Boyle, P.A., Arfanakis, K., et al., 2019. Limbic-predominant age-related TDP-43 encephalopathy (LATE): consensus working group report. Brain. 142 (6), 1503–1527.
Robinson, J.L., Lee, E.B., Xie, S.X., Rennert, L., Suh, E., Bredenberg, C., et al., 2018. Neurodegenerative disease concomitant proteinopathies are prevalent, age-related and APOE4-associated. Brain. 141 (7), 2181–2193.
Sheikh, J.I.Y.J., 1986. Geriatric Depression Scale (GDS): Recent evidence and development of a shorter version. In: Brink, T.L. (Ed.), Clinical Gerontology: A Guide to Assessment and Intervention New York. The Haworth Press, NY, pp. 165–173.
Sperling, R., Mormino, E., Johnson, K., 2014. The evolution of preclinical Alzheimer's disease: implications for prevention trials. Neuron. 84 (3), 608–622.
Spreng, R.N., Turner, G.R., 2013. Structural covariance of the default network in healthy and pathological aging. J. Neurosci. 33 (38), 15226–15234.
Stern, Y., 2006. Cognitive reserve and Alzheimer disease. Alzheimer Dis. Assoc. Disord. 20 (3 Suppl 2), S69–S74.
Tazwar, M., Evia, A.M., Tamhane, A.A., Ridwan, A.R., Leurgans, S.E., Bennett, D.A., et al., 2022. Limbic-predominant age-related TDP-43 encephalopathy neuropathological change (LATE-NC) is associated with lower R(2) relaxation rate: an ex-vivo MRI and pathology investigation. Neurobiol. Aging 117, 128–138.
Teipel, S.J., Grothe, M.J., 2022. Antemortem basal forebrain atrophy in pure limbic TAR DNA-binding protein 43 pathology compared with pure Alzheimer pathology. Eur. J. Neurol. 29 (5), 1394–1401.
Teipel, S., Grothe, M.J., 2023. MRI-based basal forebrain atrophy and volumetric signatures associated with limbic TDP-43 compared to Alzheimer's disease pathology. Neurobiol. Dis. 180, 106070.
Wisse, L.E.M., Ravikumar, S., Ittyerah, R., Lim, S., Lane, J., Bedard, M.L., et al., 2021. Downstream effects of polypathology on neurodegeneration of medial temporal lobe subregions. Acta Neuropathol. Commun. 9 (1), 128.
Zarow, C., Weiner, M.W., Ellis, W.G., Chui, H.C., 2012. Prevalence, laterality, and comorbidity of hippocampal sclerosis in an autopsy sample. Brain Behav. 2 (4), 435–442.
Zielinski, B.A., Gennatas, E.D., Zhou, J., Seeley, W.W., 2010. Network-level structural covariance in the developing brain. Proc. Natl. Acad. Sci. U. S. A. 107 (42), 18191–18196.
Zielinski, B.A., Anderson, J.S., Froehlich, A.L., Prigge, M.B., Nielsen, J.A., Cooperrider, J. R., et al., 2012. scMRI reveals large-scale brain network abnormalities in autism. PLoS One 7 (11), e49172.